Check for updates

A light-mediated covalently patterned graphene substrate for graphene-enhanced Raman scattering (GERS)†

Guilin Feng, [ID] [a] Nozomu Suzuki, [b] Qiang Zhang, [a] Jiangtao Li, [a] Tomoko Inose, [ID] [c] Farsai Taemaitree, [ID] [ad] Muhammed Shameem K. M., [ID] [e] Shuichi Toyouchi, [ID] [ef] Yasuhiko Fujita, [ID] [g] Kenji Hirai [ID] [a] and Hiroshi Uji-i [ID] *[ace]

We report covalently patterned graphene with acetic acid as a new potential candidate for graphene-enhanced Raman scattering (GERS). Rhodamine 6G molecules in direct contact with the covalently modified region show an enormous enhancement (∼25 times) compared to the pristine region at 532 nm excitation. The GERS enhancement with respect to the layer thickness of the probed molecule, excitation wavelength, and covalently attached groups is discussed.

Graphene-enhanced Raman scattering (GERS) is a promising variant of surface-enhanced Raman scattering (SERS), employing two-dimensional graphene as an active substrate to enhance Raman signals from a low quantity of molecular species.[1–5] Unlike the conventional SERS, observed at metal-molecule contact interfaces, GERS demonstrates a clean and robust signal response, characterized by reduced background interference, enhanced reproducibility, and recyclability.[4] In the GERS system, graphene plays a dual role by effectively quenching auto-fluorescence and providing a uniform surface for enhanced Raman signals. This unique combination allows for easy analysis of Raman signals from adsorbed molecules exhibiting high photoluminescence (PL). It is postulated that electron transfer and energy transfer between the graphene and the adsorbed molecules are responsible for PL quenching in GERS.[4] The magnitude of the Raman enhancement in GERS likely depends on the highest occupied molecular orbital (HOMO) and lowest unoccupied molecular orbital (LUMO) of adsorbed molecules with respect to the Fermi level of graphene. Moreover, in-depth investigations have revealed that the enhancement factor (E_F) in GERS is also influenced by additional factors including the molecular structure, phonon energy associated with the specific vibrational mode, and laser energy employed.[6,7] The enhancement effect exhibits substantial improvement when the HOMO and LUMO energy levels of the probed molecule fall within the close energy vicinity of graphene's Fermi level (E_F) for a given laser excitation energy.[6–9] Consequently, there has been a recent surge in research focus on modifying the Fermi energy of the graphene substrate as a means to modulate the EF in GERS. To date, the modulation of graphene's E_F in the context of GERS has primarily been achieved through element doping using chemical vapor deposition[10] and electronic interaction *via* solution-based molecular deposition.[11] Another approach involves charge doping into graphene utilizing an electrical field device.[7] Nonetheless, these traditional modification routes lack the ability to precisely control the Fermi level of graphene at specific locations or necessitate complex fabrication procedures.

Recently, photo-induced covalent modification (PICM) has been demonstrated as a facile method to tailor the surface properties of graphene in a desired manner.[12–14] PICM enables controlled site-specific chemisorption *via* photochemical activation with sub-μm precision. The spatially confined light irradiation permits the covalent 2D patterning at user-defined regions on the graphene substrates. Additionally, the grafting density of covalently anchored molecules onto the graphene surface can be controlled by the laser irradiation time, resulting in flexible modulation of the E_F.

Herein, we report that a photo-induced covalently modified graphene (PICM-G) substrate exhibits a remarkably high GERS

[a] *Research Institute for Electronic Science (RIES) and Division of Information Science and Technology, Graduate School of Information Science and Technology, Hokkaido University, N20W10, Sapporo, Hokkaido 001-0020, Japan. E-mail: hiroshi.ujii@kuleuven.be, hiroshi.ujii@es.hokudai.ac.jp*

[b] *Department of Chemical Science and Engineering, Graduate School of Engineering, Kobe University, Rokko, Nada, Kobe 657-8501, Japan*

[c] *Institute for Integrated Cell-Material Science (WPI-iCeMS), Kyoto University, Yoshida, Sakyo-ku, Kyoto 606-8501, Japan*

[d] *Institute of Multidisciplinary Research for Advanced Materials (IMRAM), Tohoku University, 2-1-1 Katahira, Aoba-Ward, Sendai 980-8577, Japan*

[e] *Department of Chemistry, Division of Molecular Imaging and Photonics, KU Leuven, Celestijnenlaan 200F, Leuven B-3001, Belgium*

[f] *Research Institute for Light-induced Acceleration System (RILACS), Osaka Metropolitan University, Sakai, Osaka 599-8570, Japan*

[g] *Research Institute for Sustainable Chemistry, National Institute of Advanced Industrial Science and Technology (AIST), Kagamiyama 3-11-32, Higashi-Hiroshima, Hiroshima 739-0046, Japan*

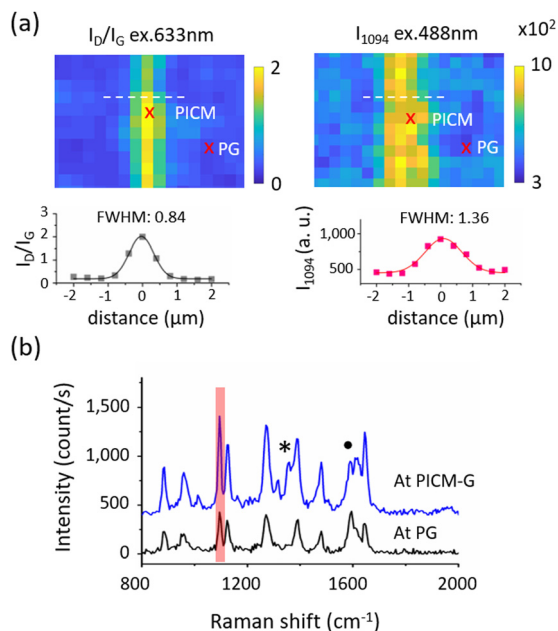† Electronic supplementary information (ESI) available. See DOI: https://doi.org/10.1039/d3cc03304j

Fig. 1 GERS of DiO molecules adsorbed on the PICM-G substrate. (a) Raman maps of I_D/I_G excited at 632.8 nm (left top) and I_{1094} excited at 488 nm (right-top), respectively. The bottom plot represents the line profile along the white dashed line. (b) Raman spectra of the DiO molecule at the pristine graphene (PG, black) and covalently patterned (blue) region excited with a 488 nm laser. The peaks marked with '*' and '•' correspond to the D and G bands of graphene, respectively. The red highlight represents the peak of DiO at 1094 cm^{-1} used for mapping.

effect on fluorescent organic molecules. PICM in acetic acid aqueous solution presents the highest GERS effect, which could be attributed to the shift of the E_F of graphene due to the covalent functionalization. For the further investigation of the GERS effect, the Langmuir–Blodgett (LB) technique was employed here to homogenously distribute the dye molecules on the graphene layer.[8,15] 3,3′-Dioctadecyloxacarbocyanine perchlorate (DiO) and rhodamine 6G (Rh6G) were selected as probe dye molecules for investigating the GERS effect.

In accordance with our previous work,[14] a 488 nm continuous wave laser was used to covalently pattern the graphene surface with chemical moieties such as –CH$_3$, –OCH$_3$, and –COOCH$_3$ (for experimental details see ESI†). A line patterned functionalization as shown in Fig. 1a was achieved by scanning the tightly focused laser (488 nm) at the interface between graphene and an aqueous solution of acetic acid (0.1 M). The photogenerated radicals are only formed in those areas where the laser is exposed to the aqueous solution resulting in a spatially controlled grafting of functional groups with the formation of sp^3 carbon defects. The Raman spectra of the PICM region with respect to the pristine graphene (PG) region are presented in Fig. S1a (ESI†). Here, a high mean intensity ratio of I_D/I_G ($>$1.2) along with the presence of the D′ peak (1619 cm^{-1}) at the shoulder of the G peak demonstrates the successful covalent modification with a high grafting density at the PICM region.[16] Consistently, the estimated full-width half-maxima (FWHM) of the PICM region (840 nm) was found to be

larger than the diffraction limit (300 nm in this study) presumably due to the diffusion of photogenerated radicals over the diffraction spot.

In our initial GERS measurements, DiO molecules (Fig. S1b, ESI†) were deposited on the PICM-G by simply immersing it in the DiO solution (1.5 mg L^{-1}) and subsequently rinsed with water to remove excess dye molecules. Raman spectra of the adsorbed dye molecules are observed from both PG and PICM-G regions, thanks to the GERS effect (Fig. 1b). However, a significantly highest signal enhancement has been clearly detected from the PICM-G region than from the PG region (Fig. 1a, right) of 1094 cm^{-1} (I_{1094}), which corresponds to one of the Raman peaks of DiO (Raman spectra of pure DiO see Fig. S2, ESI†). The FWHM of the I_{1094} map was estimated to be approximately 1360 nm, which is 1.6 times larger than that of the I_D/I_G map (Fig. 1a).

The disparity between the FWHM of the I_D/I_G ratio and that of I_{1094} could arise from the heterogeneous density of the adsorbed dye molecule and/or the GERS enhancement. To investigate the GERS effect with respect to the homogeneous distribution and number of layers of the dye molecule, the LB technique was employed. For a good signal-to-noise ratio, three layers of stearic acid labeled with DiO dyes with a molar ratio of [SA]/[DiO] $>$ 10 were used. The details are in Fig. S3–S7 (ESI†).

Fig. 2a and b display the Raman spectra of a triple LB film of DiO molecules under two different excitation wavelengths of 633 nm and 488 nm, respectively. Interestingly, no distinct Raman signature of the DiO molecule was observed when excited with 633 nm. Instead, both the PG and PICM regions exhibit Raman characteristics associated with graphene. In contrast, when excited at 488 nm, the spectra exhibit a moderate Raman signal of DiO from the PG region, while enhanced signals are observed from the PICM region. The observed difference in the GERS effect with respect to the excitation wavelength can be attributed to the fact that 488 nm is on-resonant to DiO whereas 633 nm is off-resonance (see Fig. S8, ESI†). Note that clear Raman peaks of DiO can be identified only in the presence of graphene (Fig. S9, ESI†). This indicates that the Raman enhancement is attributed to not only the resonance Raman but also to the GERS effect. The FWHM of the bright line at the I_{1094} map is estimated to be 870 nm, only 1.24 times wider than that of I_D/I_G (Fig. 2c and d), which is much narrower than the case of Fig. 1. This observation suggests that the density of the adsorbed dye molecule is relatively homogeneous between the PG and the PICM areas in the LB film compared to the simple deposition of the dye molecules by dipping graphene in the dye solution. Most importantly, the maximum of the I_D/I_G ratio map is located at the maximum of I_{1094} map. Fig. 2e shows a correlation between I_D/I_G and I_{1094}, where a higher I_D/I_G ratio results in a higher I_{1094}. This suggests that the GERS EF strongly depends on the degree of PICM on graphene.

In order to estimate the GERS effect and versatility of the newly introduced PICM graphene substrate for GERS measurement, we employed the most commonly used rhodamine 6G (Rh6G) as a probe molecule (adsorbed by immersion) and the results were compared with previously reported works. Fig. 3a depicts the Raman spectra of Rh6G on the PG and the PICM
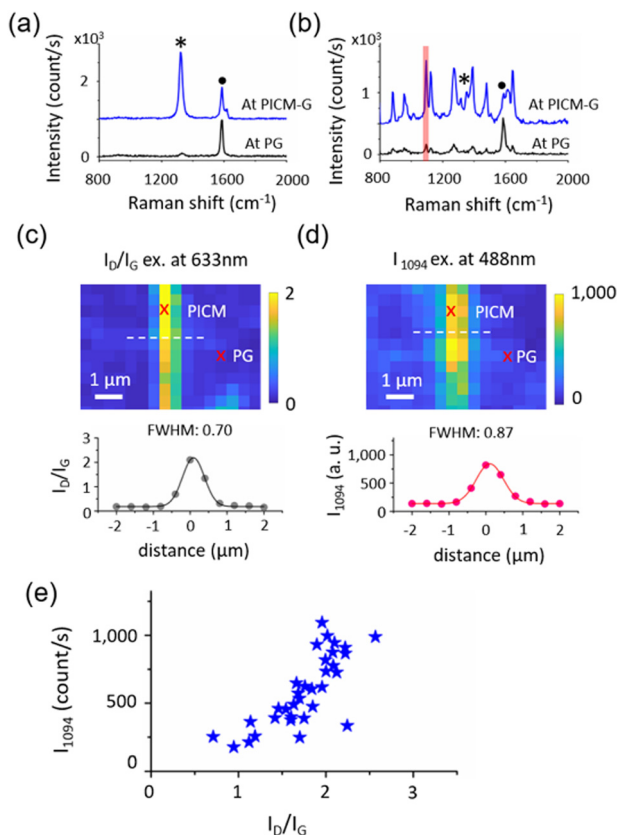
Fig. 2 Raman maps of LB films labelled with DiO on PICM-G. Raman spectra at the area of PG (black) and PICM-G (blue) excited at 633 nm (a) and 488 nm (b), respectively. The red highlight represents the peak of DiO at 1094 cm^{-1} used for mapping. (c) I_D/I_G ratio map excited at 633 nm (power: 3.08 MW cm^{-2}). (d) I_{1094} map on the same area as (c) excited at 488 nm (power: 0.78 MW cm^{-2}). The bottom plot represents the line profile along the white dashed line. (e) Correlation plot between I_D/I_G and I_{1094}. The red highlight on the Raman maps in (c) and (d) represents the regions of PICM and PG, respectively.
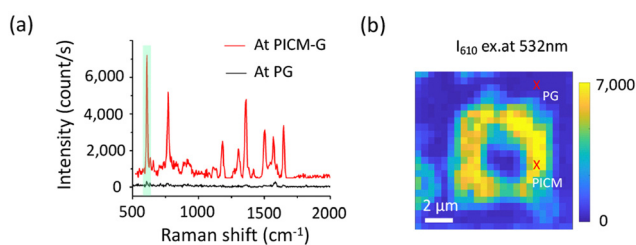

Fig. 3 (a) GERS of Rh6G on PG and PICM-G excited at 488 nm. The green highlight represents the peak of Rh6G at 610 cm^{-1} used for mapping. (b) GERS mapping of Rh6G (I_{610}, peak intensity at 610 cm^{-1}) from the PG and PICM domain under 532 nm laser excitation (0.98 MW cm^{-2}). The red crosses on the Raman maps represent the PICM and PG regions, respectively.

area under 532 nm laser excitation. Note that the fluorescence background was subtracted from the spectra (Fig. S10, ESI†). The observed Raman bands at 610, 773, 1182, 1312, 1505, and 1647 cm^{-1} are in good agreement with the earlier reports.[17] However, consistent with DiO molecules, the Raman signals are

markedly enhanced in the PICM region compared to the PG region. Furthermore, Raman mapping (Fig. 3b) and the peak ratio (I_{PICM-G}/I_{PG}) analysis (Fig. S11, ESI†) provide additional evidence of signal enhancement in the PICM region. To investigate the enhancement mechanism, we summarized the I_{1647}/I_G as a function of excitation energy, where the highest enhancement was found around 2.3 eV (Fig. S12, ESI†), indicating resonance Raman scattering effect. Considering no detectable Raman peaks of Rh6G in the absence of graphene (Fig. S13, ESI†), the GERS effect on Rh6G plays an important role. Note that electromagnetic enhancement is less likely, since the surface plasmon lies in the terahertz range rather than in the visible to NIR frequency.[6] We further analyzed the Raman shift of both G and 2D peaks at the PICM region estimating the shift tendency of graphene's E_F after the covalent modification (Table S1, ESI†).[18,19] A downshift of pos (G) indicates the electron doping effect, which could be attributed to the electron-donating properties of methyl and methoxy functionalized on graphene. As a result, the modified graphene's E_F might shift and come close to the LUMO level of Rh6G (-3.4 eV), promoting the charge transfer between the modified graphene and dye molecules. This could lead to the Raman enhancement, as suggested in the previous reports.[10,11]

It has been previously demonstrated that the type of molecule and its interaction with the graphene substrate significantly influences the GERS effect.[9] To understand the role of the different functional groups on the PICM region in GERS, different chemical groups were covalently anchored to the graphene layer with the aid of a light-triggered radical generation method. As we reported previously,[14] the PICM under an aqueous solution of acetic acid presumably introduces alkyl, ether, and ester groups on the graphene surface, while water introduces hydroxyls and oxygen species, resulting in the formation of graphene oxide. The Raman spectra of Rh6G show a very distinct enhancement value from these chemical groups as shown in Fig. S14 (ESI†). The graphene oxide displayed a small enhancement of Rh6G, whereas a significant enhancement was observed from the acetic acid functionalized area. These findings provide evidence that the functional groups within the PICM region play a critical role in determining the EF of GERS.

In Table 1, we provide a comparative summary of the GERS effect for our sample in relation to previous studies. The GERS effect was estimated by calculating the ratio of the peak intensity of the aromatic benzene ring of Rh6G at 1647 cm^{-1} (0.205 eV) from the PICM-G area to that of the PG region (I_m/I_p). Among the previously reported works, N-doped graphene exhibits the highest signal enhancement ($I_m/I_p \sim 9$) for the Rh6G molecule, while a moderate enhancement was observed from the functionalized graphene substrate with a 4-nitrophenyl group ($I_m/I_p \sim 2$). On the other hand, graphene oxide and hydrogenated graphene did not exhibit a significant enhancement at their defect sites. Remarkably, our PICM-G substrate under acetic acid exhibited an enormous signal enhancement of $I_m/I_p \sim 25$, which is an order of magnitude higher compared to other reported graphene derivatives. Our findings indicate that PICM graphene has the potential to serve as a promising candidate for future GERS substrates.

Table 1 I_m/I_p on different types of graphene substrates

Modification type	Preparation method	Dye	Laser line (nm)	Peak (cm^{-1})	I_m/I_p	Ref.
Oxide	Thermal reaction	Rh6G	532	1647	~1	20
Oxide	PICM in water	Rh6G	532	1647	~1	This work
Hydrogenated	Thermal reaction	Rh6G	532	1647	~1	21
Covalent bond with 4-nitrophenyl	Diazonium reaction	Rh6G	532	1647	~2	11
N-doped	Atom substitute	RhB	532	1647	~9	10
Covalent bond with acetic acid	PICM	Rh6G	532	1647	~25	This work

In summary, we have systematically investigated the GERS effect on organic dye molecules from pristine and PICM graphene substrates to address the signal enhancement effect. The covalent patterning is selectively created using a laser writing technique, resulting in a lateral heterojunction comprising both covalent and noncovalent domains. In contrast to the pristine region, the PICM region exhibits a significantly enhanced Raman signal of the dye molecules. Likely, the upshift of the E_F of graphene can be attributed to the signal enhancement from the PICM region. Our results also demonstrate that the GERS intensity is strongly influenced by the density of the dye molecules and the degree of covalent grafting. In addition, the resonance excitation further enhances the Raman signal of the probed dye molecule on the graphene surface. Finally, the chemical nature of the addends at the PICM region has been investigated to understand the GERS effect. The PICM-G prepared in water exhibits a much lower enhancement than the PICM-G prepared in acetic acid solution, suggesting a strong effect of functional groups for the GERS effect. The results suggest that the PICM-graphene with acetic acid is a promising GERS substrate for (bio-)chemical sensing.

GF investigated the experiment and wrote the original draft. YF, NS, QZ, JL, TI, and ST reviewed and edited the manuscript. FT, KM, MS, and KH discussed the results and co-wrote the manuscript. HU supervised the research. All the authors proof-read and approved the final manuscript for submission.

Conflicts of interest

There are no conflicts to declare.

Notes and references

1 W. Xu, N. Mao and J. Zhang, *Small*, 2013, **9**, 1206–1224.
2 C. Qiu, H. Zhou, H. Yang, M. Chen, Y. Guo and L. Sun, *J. Phys. Chem. C*, 2011, **115**, 10019–10025.
3 X. Ling, J. Wu, W. Xu and J. Zhang, *Small*, 2012, **8**, 1365–1372.
4 N. Zhang, L. Tong and J. Zhang, *Chem. Mater.*, 2016, **28**, 6426–6435.
5 L. Xie, X. Ling, Y. Fang, J. Zhang and Z. Liu, *J. Am. Chem. Soc.*, 2009, **131**, 9890–9891.
6 X. Ling, L. Xie, Y. Fang, H. Xu, H. Zhang, J. Kong, M. S. Dresselhaus, J. Zhang and Z. Liu, *Nano Lett.*, 2010, **10**, 553–561.
7 S. Huang, X. Ling, L. Liang, Y. Song, W. Fang, J. Zhang, J. Kong, V. Meunier and M. S. Dresselhaus, *Nano Lett.*, 2015, **15**, 2892–2901.
8 X. Ling and J. Zhang, *Small*, 2010, **6**, 2020–2025.
9 H. Xu, Y. Chen, W. Xu, H. Zhang, J. Kong, M. S. Dresselhaus and J. Zhang, *Small*, 2011, 7, 2945–2952.
10 S. M. Feng, M. C. dos Santos, B. R. Carvalho, R. T. Lv, Q. Li, K. Fujisawa, A. L. Elias, Y. Lei, N. Perea-Lopez, M. Endo, M. H. Pan, M. A. Pimenta and M. Terrones, *Sci. Adv.*, 2016, **2**, e1600322.
11 V. Valeš, P. Kovaříček, M. Fridrichová, X. Ji, X. Ling, J. Kong, M. S. Dresselhaus and M. Kalbáč, *2D Mater.*, 2017, **4**, 025087.
12 S. Toyouchi, M. Wolf, G. Feng, Y. Fujita, B. Fortuni, T. Inose, K. Hirai, S. De Feyter and H. Uji-i, *J. Phys. Chem. Lett.*, 2022, **13**, 3796–3803.
13 K. F. Edelthalhammer, D. Dasler, L. Jurkiewicz, T. Nagel, S. Al-Fogra, F. Hauke and A. Hirsch, *Angew. Chem., Int. Ed.*, 2020, **59**, 23329–23334.
14 G. Feng, T. Inose, N. Suzuki, H. Wen, F. Taemaitree, M. Wolf, S. Toyouchi, Y. Fujita, K. Hirai and I. H. Uji-i, *Nanoscale*, 2023, **15**, 4932–4939.
15 O. N. Oliveira, Jr., L. Caseli and K. Ariga, *Chem. Rev.*, 2022, **122**, 6459–6513.
16 M. C. Rodriguez Gonzalez, A. Leonhardt, H. Stadler, S. Eyley, W. Thielemans, S. De Gendt, K. S. Mali and S. De Feyter, *ACS Nano*, 2021, **15**, 10618–10627.
17 J. Guthmuller and B. Champagne, *J. Phys. Chem. A*, 2008, **112**, 3215–3223.
18 J. E. Lee, G. Ahn, J. Shim, Y. S. Lee and S. Ryu, *Nat. Commun.*, 2012, **3**, 1024.
19 G. Velpula, R. Phillipson, J. X. Lian, D. Cornil, P. Walke, K. Verguts, S. Brems, I. H. Uji, S. De Gendt, D. Beljonne, R. Lazzaroni, K. S. Mali and S. De Feyter, *ACS Nano*, 2019, **13**, 3512–3521.
20 S. Sil, N. Kuhar, S. Acharya and S. Umapathy, *Sci. Rep.*, 2013, **3**, 3336.
21 V. Vales, K. Drogowska-Horna, V. L. P. Guerra and M. Kalbac, *Sci. Rep.*, 2020, **10**, 4516.